Int J Clin Exp Med 2020;13(5):3418-3425
www.ijcem.com /ISSN:1940-5901/IJCEM0107894

Original Article

Study on the value of DCE-MRI maximum contrast enhancement rate in the diagnosis of demyelinating pseudotumor

Xiaofeng Dou[1*], Ting Guo[2*], Weizhong Tian[1], Mei Lin[3]

Departments of [1]Radiology, [2]Central Laboratory, [3]Scientific Research, Taizhou People's Hospital Affiliated to Nantong University, Taizhou, Jiangsu Province, China. [*]Equal contributors and co-first authors.

Received January 15, 2020; Accepted February 16, 2020; Epub May 15, 2020; Published May 30, 2020

Abstract: Objective: To explore the diagnostic value and the difference between the maximum contrast enhancement rate (MCER) and apparent diffusion coefficient (ADC) in the clinical diagnosis of patients with demyelinating pseudotumor (DPT) by magnetic resonance imaging (MRI). Methods: Study subjects: Patients with primary central nervous system lymphoma (PCNSL), atypical glioblastoma (GBM), and DPT were selected for retrospective case-control analysis. Based on different types of disease, they were divided into PCNSL group (n = 27), GBM group (n = 19) and DPT group (n = 13). Dynamic contrast enhanced magnetic resonance imaging (DCE-MRI) was performed in all patients. The characteristics of DCE-MRI images of the three groups were observed and summarized, and the differences between MCER and ADC in patients of the three groups were compared. The clinical value of MCER and ADC in the diagnosis of DPT was analyzed by receiver operating characteristic (ROC) curve. Results: The lesions of PCNSL patients were mainly nodular and lumpy, while those of GBM patients were mostly nodular and cystic, and like PCNSL patents, the lesions of DPT patients were primarily nodular and lumpy. There were significant differences in terms of enhancement characteristics among the three groups (P<0.001). There were clenched fist and concave umbilical signs in PCNSL, light garland-like enhancement in GBM, and ring-like enhancement in DPT. As to ADC and MCER values, the comparison of ADC value among the three groups was as follows: PCNSL group < GBM group < DPT group, while the comparison of MCER value was DPT < GBM < PCNSL. The ADC value and MCER value of PCNSL group and GBM group were statistically different from those of DPT group (P<0.001), while no significant difference was found between the former two groups (P>0.05). On the basis of ROC curve analysis, the AUC of the MCER value (0.982) was higher than that of ADC value (0.890). According to Youden index, the optimal threshold of ADC value for DPT diagnose was 1.07×10^{-3} mm^2/s, and that of MCER value for DPT diagnose was 71.81%. With the optimal threshold as the diagnostic threshold, the sensitivity of ADC value and MCER value was both 100%, but the specificity of MCER value (95.70%) was higher than that of ADC value (71.70%). Conclusion: DCE-MRI is of high value in the clinical diagnosis of DPT, and can be better distinguished from PCNSL and GBM through imaging characteristics, MCER and ADC values. While compared with ADC value, MCER value shows greater superiority in the clinical diagnosis of DPT, which is mainly reflected in the AUC of ROC curve analysis, and is worthy of reference in clinical diagnosis.

Keywords: MRI, demyelinating pseudotumor, maximum contrast enhancement rate, apparent diffusion coefficient, atypical glioblastoma, central nervous system lymphoma

Introduction

Demyelinating pseudotumor (DPT) is a rare inflammatory lesion of the central nervous system [1, 2], which was first reported by Velden in 1979 while studying multiple sclerosis (MS) [3]. Similar to other central space-occupying lesions, DPT patients can develop fever, dizziness, vomiting, visual impairment, speech impairment, dyskinesia, and other pathological changes such as nerve fiber demyelination and inflammatory cell infiltration around small blood vessels [4, 5]. Even today, it is still controversial whether DPT is a clinically independent disease type. Most current studies have classified it as an independent intermediate type between acute disseminated encephalomyelitis and MS [6]. Although DPT has a good clinical prognosis,

patients with delayed diagnosis can further develop into MS and lymphoma [7]. Therefore, early and effective diagnosis is of great significance to patients.

However, the dilemma we are confronting is that, due to the lack of specificity of clinical symptoms and signs of DPT, plus the early diagnosis and hormone therapy of patients can achieve a good clinical prognosis, pathological diagnosis as an invasive diagnosis is not highly accepted by patients [8]. Therefore, exploring non-invasive clinical diagnostic methods is of great significance for DPT patients. MRI is now one of the most important methods for diagnosing intracranial soft tissue diseases. By acquiring ADC value after enhanced scanning, a variety of benign and malignant tumors can be diagnosed. In recent years, the research on the application value of DCE-MRI sequences in the clinical diagnosis of intracranial soft tissue has been constantly proposed, but there is still controversy about the difference in the clinical diagnosis of benign and malignant intracranial tumors between DWI sequences and DCE sequences [9, 10]. Moreover, as the most important observation indicator of DCE-MRI sequence, the diagnostic value of MCER value in DPT still lacks controlled studies.

Therefore here, we creatively designed a controlled study to compare the value of DWI and DCE-MRI sequence scanning in the diagnosis of DPT, and quantified the examination. In addition, we applied ROC curve analysis to verify the difference between ADC value and MCER value in the diagnosis of DPT.

Materials and methods

General information

Patients with PCNSL, GBM and DPT admitted to Taizhou People's Hospital Affiliated to Nantong University from January 2017 to July 2019 were selected as the research subjects. Inclusion criteria: (1) The diagnosis of PCNSL, GBM and DPT patients was confirmed by two senior clinical pathologists [4, 5]; (2) All patients underwent MRI and enhanced scanning before receiving surgical treatment; (3) Patients with complete clinical and imaging data. Exclusion criteria: (1) Patients who received hormone therapy before MRI; (2) Patients who received surgical treatment before MRI; (3) Patients with mental retardation or mental illness that could not cooperate with the examination or treatment; (4) Patients who were allergic to contrast agents and could not perform enhanced scanning. According to the inclusion and exclusion criteria, 27 cases of PCNSL, 19 cases of GBM and 13 cases of DPT were included.

This study was approved by the Medical Ethics Committee of Taizhou People's Hospital Affiliated to Nantong University, and written informed consent was obtained from all patients and their families.

Methods

Conventional MRI, enhanced scanning and image analysis

MRI examination: Signa 1.5T dual-gradient superconducting magnetic resonance scanner (GE, USA) was applied. T1WI: TR 4-5 ms, TE 2-3 ms, flip angle 12°, field of view (FOV) 320 mm × 320 mm, layer thickness 1-2 mm, layer space 0-0.5 mm, matrix 336 × 336; T2WI: TR 3000-3500 ms, TE 120-130 ms, echo chain length of precision frequency inversion recovery sequence: 11-27, flip angle 90°, matrix 256 × 256, FOV 260 mm × 320 mm, layer thickness 3-4 mm, layer space 0-0.5 mm, matrix 512 × 512. Chopper method or hybrid method was adopted for chemical shift fat suppression technology, and it was excited twice. DWI: fast spin echo (FSE) sequence plain scan, b = 50, 800 s/mm^2, TR 2000-3000 ms, TE 100-120 ms, FOV 320 mm × 320 mm, layer thickness 4-5 mm, interval 0.5-1.0 mm, FOV 320 mm × 320 mm, excitation times 2-4.

ADC value calculation [11]: The DWI images were transmitted to a computer-aided diagnosis platform Firevoxel (FireVoxel; Center for Advanced Imaging Innovation and Research (CAI2R), New York University School of Medicine, New York, USA). ADC images of the region of interest (ROI) were measured by two staff members to calculate the ADC value. Three fields were measured and the mean value was taken as the final ADC value. One of the two staff members was responsible for calculation, and the other was in charge of review, and the work was carried out in a cross-cutting manner.

DCE-MRI scan and image analysis

DCE-MRI: After plain scanning, the contrast agent GD DTPA (BioPAL, Inc., USA) was injected

intravenously through the forearm vein at 0.2 mg/kg body weight, followed by rapid injection of 20 mL of normal saline. Before and the moment after injection, 64, 128, 191, 255, 318 s fast gradient echo sequence scanning was performed. TR 4-5 ms, TE 2-3 ms, flip angle 12°, FOV 320 mm × 320 mm, layer thickness 1-2 mm, layer space 0-0.5 mm, matrix 336 × 336, total scanning time: 7 min and 7 s.

MCER value calculation [12]: DCE-MRI images were transmitted to Mean-Curve software, the signal intensity peak (SImax) and unenhanced signal intensity (SI0) were measured, and the MCER value (MCER = (SImax-SI0) × 100%/SI0) was calculated.

Outcome measures

MRI imaging characteristics of the three groups of patients

Described the morphology of the mass according to the imaging characteristics, including nodular, mass, and cystic; Described the enhancement characteristics of the mass based on the enhanced scan images, including enhanced characteristics, clenched fist sign, concave umbilical sign, garland-like enhancement, and open-loop enhancement.

Comparison of the ADC value among the three groups

The ADC value of PCNSL, GBM and DPT patients was calculated according to the calculation formula.

Comparison of the MCER value among the three groups of patients

The MCER value of patients with PCNSL, GBM, and DPT was calculated according to the calculation formula.

Comparison of the diagnostic value of MCER and ADC in DPT

PCNSL and GBM were defined as negative and DPT was defined as positive. The clinical value of MCER and ADC in the diagnosis of DPT was analyzed by ROC curve, and the threshold value of MCER and ADC diagnosis were calculated based on Youden index. Besides, the corresponding diagnostic sensitivity and specificity of MCER and ADC diagnostic thresholds were evaluated.

Statistical analysis

Statistical analysis was performed using SPSS 24.0 (SPSS Inc., Chicago, IL, USA). The counting data, represented by patient's gender, disease course and clinical manifestations, were expressed as number of cases (percentage) [n (%)], and tested by a chi-square test, with bilateral $\alpha = 0.05$ as the test level. While mean ± standard deviation was employed to represent the measurement data such as MCER and ADC values. The inter-group comparison was performed by an independent sample t test with bilateral $\alpha = 0.05$ as the test level, while the comparison among the three groups was conducted by the F test. $P<0.05$ was considered to be statistically significant. ROC curve analysis was used to evaluate the clinical value of MCER and ADC values in the area of interest in diagnosing DPT. The area under the curve (AUC) >0.5 was evaluated as superior to random guess, indicating that it had predictive value, and the higher the AUC value, the greater the predictive value. Youden index = sensitivity + specificity-1. The maximum test result variable value of Youden index was the optimal threshold value. The optimal thresholds of MCER and ADC values were taken as the diagnostic thresholds, the above/below optimal thresholds were determined as positive, and vice versa, and their sensitivity and specificity were calculated. Sensitivity = number of true positives/(number of true positives + false negatives) × 100%; Specificity = number of true negatives/(number of true negatives + false positives) × 100%.

Results

Baseline information

There were no significant differences in the baseline data of patients regarding age, gender, course of disease or clinical manifestations between the three groups ($P>0.05$) (**Table 1**).

Differences in image characteristics of PCNSL, GBM and DPT

The lesions of PCNSL patients and DPT patients were mainly nodular and lumpy, while those of GBM patients were mostly nodular and cystic. However, no significant differences were observed in tumor morphology among patients

Table 1. Comparison of baseline information

Group	PCNSL group (n = 27)	GBM group (n = 19)	DPT group (n = 13)	χ^2/F	P
Age (year)	26.9±10.8	28.8±11.0	27.6±11.3	0.618	0.531
Gender					
Male	12	10	5	0.523	0.479
Famale	15	9	8		
Single phase course of disease					
Yes	27	19	13	/	1
No	0	0	0		
Course of disease					
Acute	17	13	8	0.557	0.438
Subacute	10	6	5		
Clinical manifestations					
Fever	10	6	5	0.128	0.359
Dizziness/Vomiting	15	10	10	0.244	0.472
Visual impairment	7	5	3	0.392	0.52
Speech impairment	4	2	1	0.772	0.654
Dyskinesia	10	6	4	0.696	0.473

Note: PCNSL: primarycenter nerve system lymphoma; GBM: glioblastoma multiforme; DPT: demyelinating pseudotumor.

Table 2. Image characteristics of PCNSL, GBM and DPT

Group	PCNSL group (n=27)	GBM group (n=19)	DPT group (n=13)	χ^2	P
Tumor morphology					
Nodular	15	10	7	0.843	0.179
Lumpy	8	3	4		
Cystic	4	6	2		
Enhancement characteristics					
Clenched fist	17	1	1	4.286	<0.001
Concave umbilical	7	1	1		
Garland-like enhancement	2	12	1		
Open-loop enhancement	1	5	10		

Note: PCNSL: primarycenter nerve system lymphoma; GBM: glioblastoma multiforme; DPT: demyelinating pseudotumor.

with PCNSL, GBM and DPT (P>0.05) (**Table 2**). As to enhancement characteristics, PCNSL had clenched fist and concave umbilical signs, GBM had garland-like enhancement, and DPT had open-loop enhancement. There were significant differences in lesion enhancement characteristics among the three groups (P< 0.001) (**Table 2**).

Lesions in DPT patients presented higher ADC value and lower MCER value

The comparison of ADC value between the three groups was PCNSL group < GBM group < DPT group (**Figure 1A**). There were statistically significant differences in ADC values between patients in PCNSL group, GBM group and DPT group (0.89±0.17 vs 1.06±0.13 vs 1.18±0.11, P<0.001), while no significant difference was observed between the PCNSL group and GBM group (P>0.05) (**Figure 1A**). The comparison of MCER value between the three groups was DPT < GBM < PCNSL (**Figure 1B**). There were statistically significant differences among the PCNSL group, GBM group, and DPT group (97.36±17.81 vs 86.72±12.48 vs 59.46±10.26, P<0.001), while no significant differences were observed between the PCNSL group and GBM group (P>0.05) (**Figure 1B**).

MCER had higher value in diagnosing DPT than ADC

The value of ADC value and MCER value in diagnosing DPT was analyzed by ROC curve, which demonstrated that the AUC of MCER value (0.982) > the AUC of ADC value (0.890) (**Table 3**; **Figure 2**). According to Youden index, the optimal threshold for ADC value to diagnose DPT was 1.07 × 10^{-3} mm^2/s, and the optimal

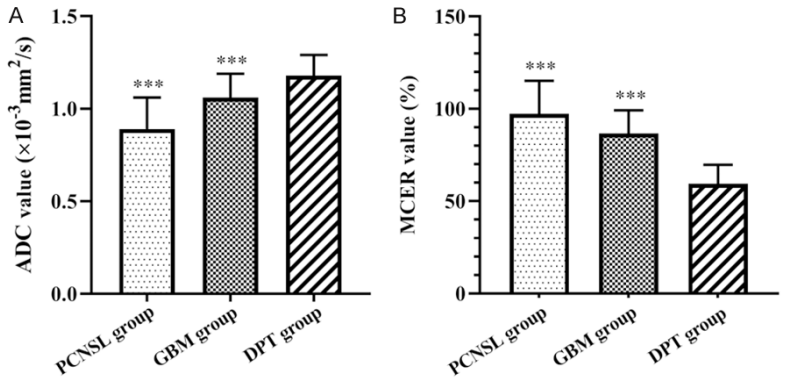

Figure 1. Comparison of ADC value and MCER value between the three groups. A. Comparison of ADC value for three group PCNSL group < GBM group < DPT group; B. Comparison of MCER value for three group DPT < GBM < PCNSL; Comparison of DPT group, ***P<0.001; ADC: apparent diffusion coefficient; MCER: maximum contrast enhancement rate; PCNSL: primarycenter nerve system lymphoma; GBM: glioblastoma multiforme; DPT: demyelinating pseudotumor.

Table 3. The value of ADC value and MCER value in diagnosing DPT

Group	AUC	Youden index	Optimal threshold	Sensitivity	Specificity
ADC value (× 10^{-3} mm^2/s)	0.89	0.717	1.07	100%	71.70%
MCER value (%)	0.982	0.957	71.81	100%	95.70%

Note: ADC: apparent diffusion coefficient; MCER: maximum contrast enhancement rate; DPT: demyelinating pseudotumor.

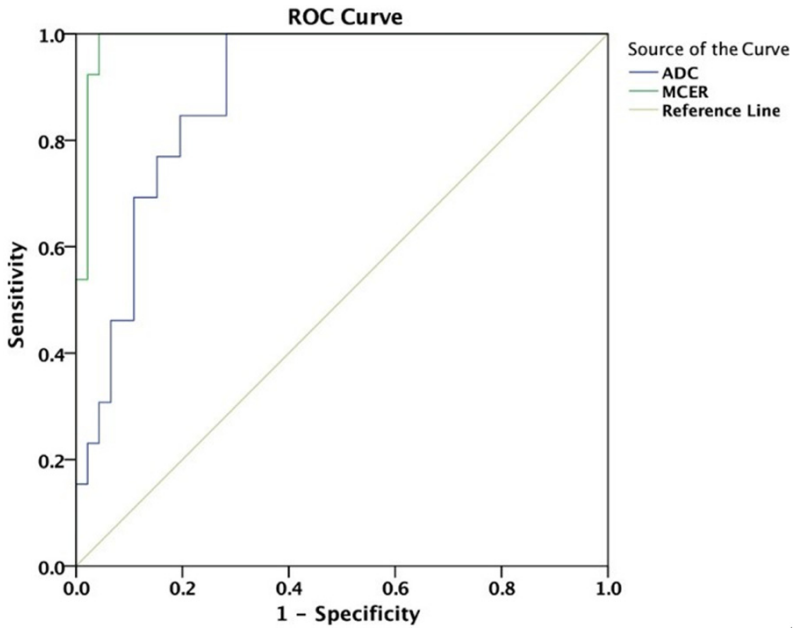

Figure 2. The ROC curve of ADC value and MCER value diagnosis DPT. ROC: receiver operating characteristic; ADC: apparent diffusion coefficient; MCER: maximum contrast enhancement rate; DPT: demyelinating pseudotumor.

threshold for MCER value to diagnose DPT was 71.81%. With the optimal thresholds as the diagnostic thresholds, the sensitivity of ADC value and MCER value was both 100%, but the specificity of MCER value (95.70%) was higher than that of ADC value (71.70%) (**Table 3**; **Figure 2**).

Discussion

Magnetic resonance imaging (MRI) is currently one of the most effective diagnostic methods for brain glioma by placing the examination site in a static magnetic field and giving specific radio frequency pulses to stimulate hydrogen protons in human body to generate resonance. After the pulse is stopped, MR signals during proton relaxation are received and images are reconstructed [13, 14]. PCNSL, GBM and DPT are all regarded as brain soft tissue lesions, and MRI observation of their imaging characteristics has clinical value in the diagnosis and treatment of these diseases [9, 10, 13, 14].

After MRI examination of the three groups of patients, it was found that the three diseases had no significant difference in the morphology of the target area, but showed significant differences in the characteristics of the enhanced signal. The main manifestations of PCNSL, GBM, and DPT were nodular, mass, and cystic, and it was not feasible to diagnose the disease by the morphology of lesions. In terms of enhancement characteristics, 10 out of 13 DPT patients exhibited open-loop enhancement, which should be identified with the garland-like enhancement in

GBM patients. The study of Tremblay showed that, because demyelination of nerve fibers in DPT patients often occurred in the white matter of the brain, ring formation was enhanced at the edge of the lesion, while the myelin sheaths in the gray matter part and the basal part rarely form a gap, hence the MRI characteristics of DPT patients showed open-loop enhancement, which was in line with the results of this study [15]. While the first sign and concave umbilical sign of patients with PCNSL are more easily distinguished from it [16, 17]. This result indicates that it is possible to differentiate between PCNSL, GBM and DPT by enhanced characteristics in clinical diagnosis, except that the diagnostic results place higher requirements on radiograph readers, and there may be a high error rate. As for PCNSL and GBM, the similar cell density and growth pattern of their lesions result in the difficulty to diagnose and differentiate between PCNSL, GBM and DPT by MRI imaging characteristics, so it is necessary to use quantitative analysis to diagnose DPT [18].

DWI can reflect the diffusion of water molecules in tissues through ADC value, and can thus evaluate the structure and internal changes of lesion tissues. ADC value is positively correlated with the motility of water molecules, and the lower ADC value is, the worse the motility of water molecules is. The diagnostic value of ADC value calculated by DWI in benign and malignant lesions has been proved in many clinical fields, including brain tissue, breast, liver, thyroid nodules [19]. Back in 2002, Lin retrospectively analyzed 7 pathologically confirmed DPT of the central nervous system and 1 clinically confirmed MR image [20]. The results showed that it was a difficult task to correctly diagnose DPT of central nervous system based on clinical data and imaging findings, which was often misdiagnosed as tumor by MRI. A meta-analysis conducted by Lu demonstrated that DWI had a higher value in the differential diagnosis of PCNSL and GBM, and the quantitative detection of ADC value could be used for the differential diagnosis of PCNSL and GBM [21]. However, there are also shortcomings in the quantitative detection of ADC value, which are not only affected by the number, size, arrangement, and extracellular space of cells, but are also related to nuclear-plasma ratio, number of organelles, and microcirculation. The case report of Ning described the diagnosis and treatment of DPT in patients who were initially misdiagnosed as astrocytoma, with higher ADC value in DPT patients, and suggested that correct diagnosis of DPT can avoid blind surgery [22]. However, as mentioned earlier, the incidence of DPT is quite low, as a result, the reports on the diagnosis of DPT with ADC value are very limited, especially the controlled studies with other intracranial lesions. The results of this study showed that there were significant differences in ADC value of PCNSL, GBM and DPT patients, and the ROC curve analysis indicated that ADC value enjoyed higher value in clinical diagnosis of DPT patients. The reason may be that DPT patients have a low degree of restricted diffusion of water molecules, which is the characteristic of benign lesions, and this result is also consistent with the characteristics of precursor lesions [6].

DCE-MRI is a new discovery of MRI technology in recent years. Unlike traditional MRI, which can only explain the tissue enhancement at a certain time point, DCE-MRI can obtain a series of continuous dynamic enhancement images that can reflect the tissue enhancement in various periods before, during and after contrast agent injection through continuous and fast imaging sequences, and can effectively reflect the microcirculation function of lesion tissues through software quantitative analysis [23, 24]. Moreover, it has a lower dependence on field strength, and can be scanned at a field strength of 1.5T, so it has a higher application scenario. DCE-MRI is currently used in the diagnosis and prognostic evaluation of a variety of clinical diseases. Among them, MCER has attracted extensive attention as it has a better expression of tissue blood supply and perfusion. The reason is that the MCER is determined by tissue blood supply and perfusion. MCER value is different from ADC value in that the former mainly reflects the diffusion of tissue water molecules and the nature of cells, while the latter primarily reflects the capillary permeability and the microcirculation function of the lesion tissue [25, 26]. The present study revealed that the MCER value of PCNSL, GBM and DPT patients was significantly different, presenting a gradient change of DPT < GBM < PCNS. The main reason was that the vessels in DPT lesions were less affected by endothelial cell proliferation and had a lower signal change rate, while the vascular walls of PCNSL and

GBM lesions were infiltrated by tumor cells and caused capillary endothelial hyperplasia, so the amount of contrast agent in the vessels increased, presenting a higher signal change rate [27, 28]. The comparison between MCER value and ADC value in the clinical diagnosis of DPT patients exhibited that MCER value had higher AUC and specificity than ADC value, and the reason might be that the latter was affected by cell number, size, arrangement and extracellular space.

The design of current study also has certain shortcomings. First, due to the low incidence of DPT, the number of cases available for research is small, which may cause some bias. Second, only PCNSL and GBM were included, without comparison with other gliomas, which is also our limitation. Therefore, even if the results of this study are accurate, it is still necessary to further expand the sample size to determine the diagnostic value of MCER value in DPT.

In summary, by contrast with MRI images of PCNSL and GBM, we found that the lesion morphology of DPT patients was mainly nodular and clump, and presented the characteristics of open-loop enhancement, which could be used as a reference in clinical diagnosis. In addition, compared with quantitative MRI analysis indexes of PCNSL and GBM, DPT patients had higher ADC value and lower MCER value. Both ADC value and MCER value had higher value in the diagnosis of DPT, and the value of the latter is better than the former.

Acknowledgements

This work was supported by the Hospital-level Project for Study on targeted therapy of PSMA-siRNA/DTX nanoliposomes based on MFH technology for prostate cancer and magnetic resonance imaging (ZL201948).

Disclosure of conflict of interest

None.

Address correspondence to: Weizhong Tian, Department of Radiology, Taizhou People's Hospital Affiliated to Nantong University, No. 366 Taihu Road, Medical High-tech Zone, Hailing District, Taizhou 225300, Jiangsu Province, China. Tel: +86-0523-86606726; Fax: +86-0523-86606726; E-mail: tianweizhongtzh1@163.com; Mei Lin, Department of Scientific Research, Taizhou People's Hospital Affiliated to Nantong University, No. 366 Taihu Road, Medical High-tech Zone, Hailing District, Taizhou 225300, Jiangsu Province, China. Tel: +86-0523-86606726; Fax: +86-0523-86606726; E-mail: linmeitzh1@163.com

References

[1] Shu Y, Long Y, Wang S, Hu W, Zhou J, Xu H, Chen C, Ou Y, Lu Z, Lau AY, Yu X, Kermode AG and Qiu W. Brain histopathological study and prognosis in MOG antibody-associated demyelinating pseudotumor. Ann Clin Transl Neurol 2019; 6: 392-396.

[2] Wen JB, Huang WY, Xu WX, Wu G, Geng DY and Yin B. Differentiating primary central nervous system lymphomas from glioblastomas and inflammatory demyelinating pseudotumor using relative minimum apparent diffusion coefficients. J Comput Assist Tomogr 2017; 41: 904-909.

[3] van der Velden M, Bots GT and Endtz LJ. Cranial CT in multiple sclerosis showing a mass effect. Surg Neurol 1979; 12: 307-310.

[4] Matias-Guiu JA, Cabrera-Martin MN, Cortes-Martinez A, Pytel V, Moreno-Ramos T, Oreja-Guevara C, Carreras JL and Matias-Guiu J. Amyloid PET in pseudotumoral multiple sclerosis. Mult Scler Relat Disord 2017; 15: 15-17.

[5] Kuo B and Singh P. Nausea and vomiting related to the central nervous system diseases. Springer International Publishing 2017.

[6] Lotan I, Brody J, Hellmann MA, Bialer O, Ganelin-Cohen E, Michaeli N, Marignier R and Stiebel-Kalish H. Myelin oligodendrocyte glycoprotein-positive optic neuritis masquerading as pseudotumor cerebri at presentation. J Neurol 2018; 265: 1985-1988.

[7] Neuronavigation-guided biopsy for differential diagnosis of pseudotumoral demyelinating brain lesions. Neurosurgery 1: 44-46.

[8] Ng S, Butzkueven H, Kalnins R and Rowe C. Prolonged interval between sentinel pseudotumoral demyelination and development of primary CNS lymphoma. J Clin Neurosci 2007; 14: 1126-1129.

[9] Gu FR, Yan XL, Qin J and Xu XL. Clinical analysis of five cases of demyelinating pseudotumor. Chinese Journal of Contemporary Neurology & Neurosurgery 2017; 17: 214-222.

[10] Huang WY, Wu G, Li JJ, Geng DY, Tan WL and Yu XR. Early prediction of functional outcome using dynamic contrast enhanced magnetic resonance imaging in experimental stroke. Magn Reson Imaging 2016; 34: 1000-1007.

[11] Bonarelli C, Teixeira PA, Hossu G, Meyer JB, Chen B, Gay F and Blum A. Impact of ROI positioning and lesion morphology on apparent dif-

fusion coefficient analysis for the differentiation between benign and malignant nonfatty soft-tissue lesions. AJR Am J Roentgenol 2015; 205: W106-113.
[12] Niedermayer S, Prompona M, Cyran CC, Reiser M and Huber A. Dose response of the intravascular contrast agent gadofosveset trisodium in MR perfusion imaging of the myocardium using semiquantitative evaluation. J Magn Reson Imaging 2014; 39: 203-210.
[13] Bakas S, Akbari H, Sotiras A, Bilello M, Rozycki M, Kirby JS, Freymann JB, Farahani K and Davatzikos C. Advancing the cancer genome atlas glioma MRI collections with expert segmentation labels and radiomic features. Sci Data 2017; 4: 170117.
[14] Calixto NC, Simao GN, Dos Santos AC, de Oliveira RS, Junior LGD, Valera ET, Cintra MB and Mello AS. Monitoring optic chiasmatic-hypothalamic glioma volumetric changes by MRI in children under clinical surveillance or chemotherapy. Childs Nerv Syst 2019; 35: 63-72.
[15] Tremblay MA, Villanueva-Meyer JE, Cha S, Tihan T and Gelfand JM. Clinical and imaging correlation in patients with pathologically confirmed tumefactive demyelinating lesions. J Neurol Sci 2017; 381: 83-87.
[16] Kim Y, Cho HH, Kim ST, Park H, Nam D and Kong DS. Radiomics features to distinguish glioblastoma from primary central nervous system lymphoma on multi-parametric MRI. Neuroradiology 2018; 60: 1297-1305.
[17] Ahn SY, Kwon SY, Jung SH, Ahn JS, Yoo SW, Min JJ, Bom HS, Ki SY, Kim HJ, Lee JJ, Song SY and Yang DH. Prognostic significance of interim 11C-methionine PET/CT in primary central nervous system lymphoma. Clin Nucl Med 2018; 43: e259-e264.
[18] Ozdemir ES, Yildirim AE and Can AY. primary central nervous system lymphoma of optic chiasma: endoscopic endonasal treatment. J Craniofac Surg 2018; 29: 199-201.
[19] Bruegel M, Holzapfel K, Gaa J, Woertler K, Waldt S, Kiefer B, Stemmer A, Ganter C and Rummeny EJ. Characterization of focal liver lesions by ADC measurements using a respiratory triggered diffusion-weighted single-shot echo-planar MR imaging technique. Eur Radiol 2008; 18: 477-485.
[20] Lin MA, Cai Y, Gao Y, Liang Y and Liang L. MRI of demyelinating pseudotumor of the central nervous system. Chinese Journal of Radiology 2002; 36: 601-604.
[21] Lu X, Xu W, Wei Y, Li T, Gao L, Fu X, Yao Y and Wang L. Diagnostic performance of DWI for differentiating primary central nervous system lymphoma from glioblastoma: a systematic review and meta-analysis. Neurol Sci 2019; 40: 947-956.
[22] Ning X, Zhao C, Wang C, Zhang D and Luo Q. Intracranial demyelinating pseudotumor: a case report and review of the literature. Turk Neurosurg 2017; 27: 146-150.
[23] Hanson E, Eikefjord E, Rorvik J, Andersen E, Lundervold A and Hodneland E. Workflow sensitivity of post-processing methods in renal DCE-MRI. Magn Reson Imaging 2017; 42: 60-68.
[24] Kostopoulos SA, Vassiou KG, Lavdas EN, Cavouras DA, Kalatzis IK, Asvestas PA, Arvanitis DL, Fezoulidis IV and Glotsos DT. Computer-based automated estimation of breast vascularity and correlation with breast cancer in DCE-MRI images. Magn Reson Imaging 2017; 35: 39-45.
[25] Deka K, Guleria A, Kumar D, Biswas J, Lodha S, Kaushik SD, Choudhary SA, Dasgupta S and Deb P. Janus nanoparticles for contrast enhancement of T1-T2 dual mode magnetic resonance imaging. Dalton Trans 2019; 48: 1075-1083.
[26] Mannucci T, Lippi I, Rota A and Citi S. Contrast enhancement ultrasound of renal perfusion in dogs with acute kidney injury. J Small Anim Pract 2019; 60: 471-476.
[27] Choi YS, Lee HJ, Ahn SS, Chang JH, Kang SG, Kim EH, Kim SH and Lee SK. Primary central nervous system lymphoma and atypical glioblastoma: differentiation using the initial area under the curve derived from dynamic contrast-enhanced MR and the apparent diffusion coefficient. Eur Radiol 2017; 27: 1344-1351.
[28] Koriyama S, Nitta M, Shioyama T, Komori T, Maruyama T, Kawamata T and Muragaki Y. Intraoperative flow cytometry enables the differentiation of primary central nervous system lymphoma from glioblastoma. World Neurosurg 2018; 112: e261-e268.